VER
Vascular & Endovascular Review

Posaconazole Loaded Quatsomes For Topical Delivery : Development And Optimization By 3^2 Factorial Design

IndiraMuzib Y [1]*, NaveenTaj. S[1], Swathi.K[1],Suvarnalatha Devi.P[2]

[1]Institute of Pharmaceutical Technology, Sri Padmavati MahilaVisvavidyalayam, Tirupati, Andhra Pradesh, India-517502.
[2]Department of Applied Microbiology, Sri Padmavati MahilaVisvavidyalayam, Tirupati, India-517502.
*Corresponding author Email: yindira1415@gmail.com

Corresponding Author's details:
Dr.Y.Indira Muzib,
Professor,
Institute of Pharmaceutical Technology,
Sri Padmavati MahilaVisvavidyalayam,
Tirupati-517502,
Andhra Pradesh, India.
Contact No.919441593292,
Email: yindira1415@gmail.com

ABSTRACT

Objective: The self-assembling quatsomes, as a new-generation nanovesicle, provide a great advantage over older lipid-based carriers such as liposomes and niosomes, as quatsomes resolve many of the limitations associated, such as chemical instability and encapsulation inefficiency. These nanostructures are created from a single-chain cationic surfactant and cholesterol. The study aimed to formulate posaconazole-loaded quatsomes while determining the impact of cetylpyridinium chloride (CPC) and cholesterol on the selected responses like particle size, entrapment efficiency, and in vitro drug release.

Method: Posconazole is BCS-II drug with the criteria low solubility and high permeability, this limitation of poorly soluble nature of the drug can enhanced by loading in proper carrier-based system like quatsomes. Posconazole loaded quatsomes was prepared by thin film hydration method and a total of nine formulations were prepared by selecting a 32 factorial design using design expert software version 13.0, which were then analyzed using response surface methodology (RSM).

Results: Statistical analysis like ANOVA was used to determine the significance of the models; $p < 0.05$ was considered as significant. All three responses were found statistically significant with R^2 being greater than 0.97. Cholesterol was found to be a highly significant factor for particle size; as increase in concentration of lipid resulted in increased particle size. For entrapment efficiency, the significant factors like CPC and cholesterol, increase in cholesterol level was found to decrease efficiency. Through the obtained results it was concluded that selected factors shows a major impact on responses.

Conclusion: Out of all nine formulations, F3 for which a desirability function was maximized contained 100mg of cationic surfactant CPC and 150 mg of cholesterol. These particles in optimized formulation found to be with a size of 133.7nm, 93.68% entrapment efficiency, and 92.5% invitro drug release.

KEYWORDS: Novel carrier, enhanced permeability, Optimization, drug release, quatsomes

How to Cite: IndiraMuzib Y, NaveenTaj. S, Swathi.K, Suvarnalatha Devi.P., (2025) Posaconazole Loaded Quatsomes For Topical Delivery : Development And Optimization By 3^2 Factorial Design, Vascular and Endovascular Review, Vol.8, No.19s, 252-263

INTRODUCTION

Vesicular systems are advanced drug delivery carriers made of lipid bilayers that form spherical, vesicle-like structures capable of encapsulating both hydrophilic and lipophilic drugs. These systems, which include liposomes, niosomes, transfersomes, ethosomes and quatsomes, are proven to be to enhance drug stability, improve bioavailability, and allow controlled or targeted release to specific tissues. By mimicking biological membranes, vesicular systems protect drugs from degradation, reduce toxicity, and improve therapeutic effectiveness. Their versatility makes them widely used in pharmaceutical, cosmetic, and biomedical applications [1].

One such novel carrier like quatsomes are an example of an innovative development in the nano vesicular drug delivery system technology, and are a potential substitute for the traditional lipid carriers such as liposomes and niosomes[2]. Quatsome defined as self-assembling vesicles formed from the combination of a single-chain cationic surfactant with cholesterol,they are formed

from the conjunction of “quaternary ammonium” and “liposome” due to their vesicle’s characteristics[3,4].Drug delivery in vesicular systems started with the use of liposomes in the1960’s.The liposomes are a single phospholipid bilayer wrapped in a phospholipid bilayer structure forming vesicles that hydro and lipophobic. The encapsulated drug delivery systems liposomes are able to foe with, which is hydrophobic or hydrophilic [5,6]. The issues with the use of liposomes are peculiarly high and unreasonable for the rest of the market the cost of production, as well as the inexpensive and efficient chemical reactions liposomes undergo are challenges. These systems are prone to oxidation, and are undertaken quickly by the reticuloendothelial system, thus many attempted to use niosomes, which are superior to liposomes and which are formed from non-ionic surfactants. Even though niosomes are more stable and more cost effective than liposomes, they still have limitations around drug encapsulation effectiveness and membrane and drug leakage[7].The self-assembly of cetylpyridinium chloride (CPC) and cholesterol gives rise to quatsomes[8]. The positive polar region of cationic single-chain surfactants, unlike liposomes which have double-chain phospholipids, is very large[9,10]. These polar head groups naturally repel each other, making the formation of a vesicle impossible. Insertion of cholesterol which serves as a "spacer" in the membrane neutralizes the positive charge and thus enables the formation of stable vesicles. The cationic surfactant and cholesterol together in a quatsome create more resistance to breakdown [11].

The making of quatsomes is prepared by using the thin film hydration method[12,13].These methods great ease in formulating makes quatsomes a suitable carrier for loading poorly soluble drugs[14].The formulated quatsomes should be small, uniform in size, and perfect for systemic circulation and cellular uptake ranging from 50 to 200 nanometers and for local action as topical delivery with low molecular weight drugs[15].Another major positive trait is the positive surface charge of the quatsomes, promoting contact with biological membranes and macromolecules for targeted delivery[16-18].

Posaconazole is a type of N-arylpiperazine characterized by a piperazine ring substituted at both the 1 and 4 positions with 4-substituted phenyl groups[19,20]. It belongs to the class of triazole antifungal agents and also exhibits trypanocidal activity. Structurally, it falls under several chemical categories, including triazoles, N-arylpiperazines, organofluorine compounds, oxolanes, aromatic ethers, and azole antifungals[21,22].

Posaconazole, a second-generation triazole antifungal, shows broad-spectrum activity and has been effective in treating fungal keratitis[23]. However, its poor water solubility reduces bioavailability and therapeutic efficiency. Commercially, PSC is available in oral suspension, infusion, and tablet forms, but no gel formulation exists [24].

The selected research was focused on formulation, optimization and characterization of a poorly soluble drug like posconazole into a novel carrier like quatsomes to overcome its drawbacks like low solubility by selecting3^2factorial experimental design. A total of nine formulations were generated by design and were subjected to characterization.

MATERIALS AND METHODS

Materials: Posaconazole (Drug) was a gift sample and Cetylpyridinium chloride (CPC) Cholesterol, Ethanol, PVA were procured from himedia chemicals. All the solvents used in the study are of analytical grade.

Method:

Formulation of Posaconazole loaded Quatsomes

The formulation of posconazole loaded Quatsomes by thin film hydration by using rotary evaporator [25,26].The organic phase was prepared by dissolving cetylpyridinium chloride (CPC), cholesterol, and posaconazole in a suitable organic solvent like ethanol for optimization of bilayer stability [27,28].The lipid concentration selected from 100 to 200mg, depending on their desired vesicle yield and drug loading. An aqueous phase was prepared by dissolving 100

mg of polyvinyl alcohol (PVA) in purified water to obtain a 0.1% (w/v) solution. This solution served as both a stabilizer and hydration medium during quatsome formulation. Then the organic phase was added dropwise into the aqueous PVA solution with continuous stirring at room temperature. The quatosomes was homogenized by using a high-speed homogenizer at rpm of 2,000–10,000 for 15-30 min [29]. The rate of addition was controlled to ensure the uniform dispersion and formation of a quatsomes. The resulting quatsome formulation was stored at 4°C in a vial until further characterization.

Characterization of Quatsomes [30-32]

Particle size and Zeta potential: The particle size, zeta potential was assessed using zetasizer (Malvern Instruments, UK). A sufficient sample was dispersed in distilled water and measured all the parameters at 25°C. The parameters were measured based on the intensity of light scattered and conductivity of quatsomes.

Entrapment Efficiency (%): The quatsomes loaded drug was assessed to evaluate the entrapment efficiency. About 2 mL of formulation was solubilized in 5mL of ethanol and centrifuged the suspension at 10,000 rpm for 15 min. Then the supernatant liquid was filtered using a membrane filter and the drug concentration was analysed using a UV-vis spectrophotometer at 260nm. The percentage entrapment efficiency was calculated by following formula;

Entrapment Efficiency (%) = (Amount of Drug Entrapped / Total Amount of Drug Used) x 100

***In vitro* Drug Release**

The drug loaded quatsomes was taken in a dialysis tube and donor chamber was safely clamped using strings. Soaking the dialysis membrane overnight in PBs (pH 7.4, release medium) to reach equilibrium was done. Afterwards, a volume enclosing the optimum formula was placed in the bag positioned in an amber bottle enclosing 50 ml of release medium. About 2.0 mL of

sample was collected at predefined intervals upto 8 hr and the fresh solvent replaced to maintain sink conditions. The amount drug released was measured by UV spectroscopy at of 260 nm.

Drug excipient compatibility studies

Fourier Transform Infrared (FTIR) Spectroscopy

FTIR spectroscopy was performed to identify potential drug-polymer interactions using an FTIR spectrophotometer. Samples of pure posaconazole and the optimized quatsomal formulation were individually mixed with potassium bromide in a 1:100 ratio and compressedinto transparent pellets using a hydraulic press at 10 tons pressure for 5 minutes. The FTIR spectra were recorded in the wave number range of 4000-400 cm^{-1} with a resolution of 32 scans per sample. The characteristic peaks of the drug and formulation were identified and compared to assess any chemical interactions or compatibility issues.

Powder X-ray diffraction (PXRD)

A powder X-ray diffractometer (Ultima IV, Rigaku, Japan) was used to record the scattering pattern of the sample using Cu-Kα X-radiation (λ = 1.54 Å) at 40 kV and 30 mA power. The sample was spread uniformly on a quartz plate. The scattering pattern of pure drug and optimized formulation was recorded over a scanning range of 5◦ to 50◦ 2h at 0.045step/0.5s.

Differential scanning calorimetry (DSC)

The amorphous nature of the drug distributed in the lipid was determined using differential scanning calorimetry tests. The Mettler Toledo DSC 8220 instrument was used to conduct DSC analysis of posaconazole and Optimized formulation. To ensure an inert atmosphere, samples were weighed in an aluminium pan and regulated at temperatures ranging from 0 to 800°C at a scanning rate of 10°C/min.

Surface Morphology by Scanning electron microscopy and Phase Contrast Microscopy

The phase contrast microscopy study was carried out to examine the morphology and vesicular characteristics of the prepared quatsome formulation. A small drop of the diluted sample was placed on a clean glass slide, gently covered with a coverslip, and observed under phase contrast microscope equipped with suitable phase objectives (10×, 40× and 100×).The microscope was adjusted using Köhler illumination for even light distribution. The quatsome vesicles appeared as distinct spherical structures surrounded by bright and dark halos, confirming their uniformity and structural integrity. Images were captured using a digital camera attached to the microscope for detailed analysis of particle shape and uniformity.

RESULTS AND DISCUSSION

Optimization of prepared formulations using 3^2factorial experimental design

A systematic approach was used to optimize the formulation by exploring the relationship between the selected independent variables and the observed responses. A total of nine formulations were prepared according to the 3^2factorial experimental design, and their characterized were analyzes for various responses, including particle size, entrapment efficiency, and *invitro* dug release. Response surface methodology (RSM) was employed to understand the effect of the selected independent variables on the observed responses. The importance of the experimental model was evaluated through an ANOVA, lack of fit, and the multiple correlation coefficients (R2) as shown in Table 1.

The mathematical relationship between the factors and responses was established and fitted to a second-order polynomial equation. For the model to be considered statistically significant, the p-value was required to be less than 0.05.

The coefficients of the second-order polynomial equation were analyzed to determine the impact of each factor and their interactions. This analysis revealed that the responses were quadratic in nature with significant interactive terms, confirming a complex relationship that cannot be described by simple linear models. The final optimized formulation was identified by applying a desirability function to simultaneously achieve the target values for all responses.

Table 1: Selection of dependent and independent variables

	Independent variables		**Dependent variables**		
Run	A:CPC	B:CHOLESTEROL	ParticleSize (nm)	Entrapment Efficiency (%)	*Invitro* Drug Release
	mg	**mg**	**nm**	**%**	**%**
1	100	100	134.9	89.9	89.6
2	50	100	145.4	84.39	84.9
3	100	150	133.7	93.68	92.5
4	50	200	232.3	73.21	86.7
5	100	200	286.6	79.8	92.0
6	150	200	295.2	84.7	87.9
7	150	100	142.7	86.89	91.2
8	150	150	148.2	87.1	88.4
9	50	150	145	86.89	82.8

Statistical analysis for Particle size: Statistical analysis was carried out to know the significant effect of independent variables on the response.

Contour ploplots and response surface for particle size

Two-dimensional contour plots and three-dimensional counter plots were constructed to elucidate the relationship between the independent and dependent variables. These types of plots are useful for studying the interaction effects, between two factors and for understanding how the effect of one factor will be influenced by the change in the level of another factor.

Polynomial equation

Particle size **= +142.72 + 10.57(A) + 65.50(B) + 16.40(AB) - 0.0333(A^2) + 63.17(B^2)**.

The polynomial equation obtained represents the sign indicates collegial effect and negative sign indicates opposing effect of the independent variables on the response In this equation, A represents the coded level of CPC and B represents the coded level of Cholesterol.The coded factors can be used to compare the relative impact of each factor.The positive coefficient for B (+65.50) indicates that as the amount of cholesterol increases, the particle size also increases. The large magnitude of this coefficient, compared to the others, shows that cholesterol has the most significant impact on the particle size.

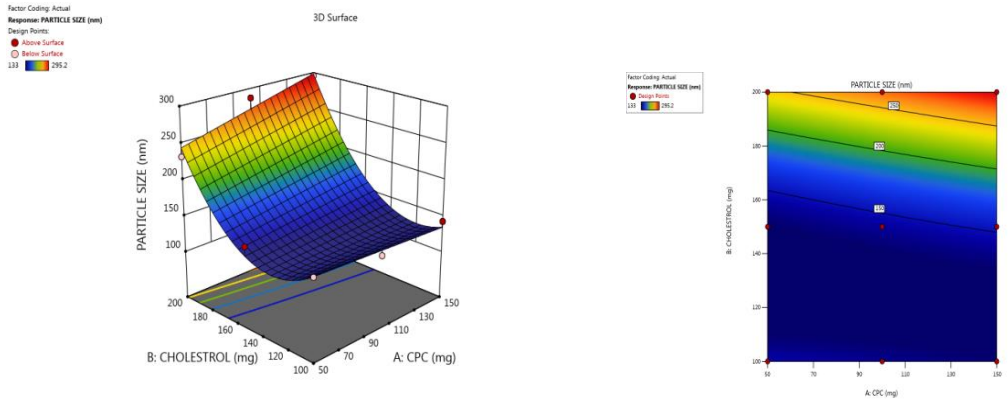

Fig 1:2D surface plot and 3D contour plot for Particle size

The contour plot for Particle Size visually represents how changes in the two factors, CPC (Factor A) and Cholesterol (Factor B), affect the resulting particle size, as shown in figure 1.

Effect of Cholesterol: The contours or lines of constant particle size, on the plot are closely arranged along the y-axis (B: CHOLESTEROL). This tight spacing indicates a steep gradient, meaning a small change in cholesterol concentration results in a large change in particle size. The color gradient also shows this relationship, with the deepest blue region (indicating the lowest particle size) at low cholesterol levels and the red/orange region (indicating the highest particle size) at high cholesterol levels. This strong influence is confirmed by the ANOVA table, where the p-value for Cholesterol (B) and its quadratic term (B^2) are statistically significant ($p < 0.05$).

Effect of CPC: In contrast, the contours are considerable spaced along the x-axis (A: CPC). This wide spacing shows that the particle size is much less sensitive to changes in the CPC concentration. The ANOVA results support this, as the p-value for CPC (A) is 0.0202 which is statistically significant ($p<0.05$).

Table 2: Statistical analysis for Particle size

Source	Sum of Squares	Df	Mean Square	F-value	p-value	Inference
Model	35467.32	5	7093.46	27.93	0.0102	Significant
A-CPC	669.93	1	669.93	2.64	0.0202	
B-CHOLESTROL	25741.50	1	25741.50	101.35	0.0021	
AB	1075.84	1	1075.84	4.24	0.1317	
A^2	0.0022	1	0.0022	8.750E-06	0.9978	
B^2	7980.06	1	7980.06	31.42	0.0112	
Residual	761.94	3	253.98			
Cor Total	36229.27	8				

Model Significance: The model's F-value is 27.93, with a p-value of 0.0102, which is less than 0.05. This indicates that the model is significant and that there is only a 1.02% chance this F-value is due to noise.

Significant Factors:

The individual factors with a p-value of less than 0.05 are considered significant.B-Cholestrol has a p-value of 0.0021, making it a highly significant factor.B^2 (Quadratic term for Cholesterol) has a p-value of 0.0112, which is also significant.

Fit Statistics:

The model's R^2 is 0.9790, meaning it explains approximately 97.9% of the variability in the particle size.The Adequate Precision ratio is 12.7725, which is well above the desirable value of 4, indicating an adequate signal and that the model can be used to navigate the design space.

In summary, the contour plot clearly demonstrates that particle size is predominantly driven by the concentration of cholesterol, and to obtain a smaller particle size, it is necessary to use lower concentrations of cholesterol.

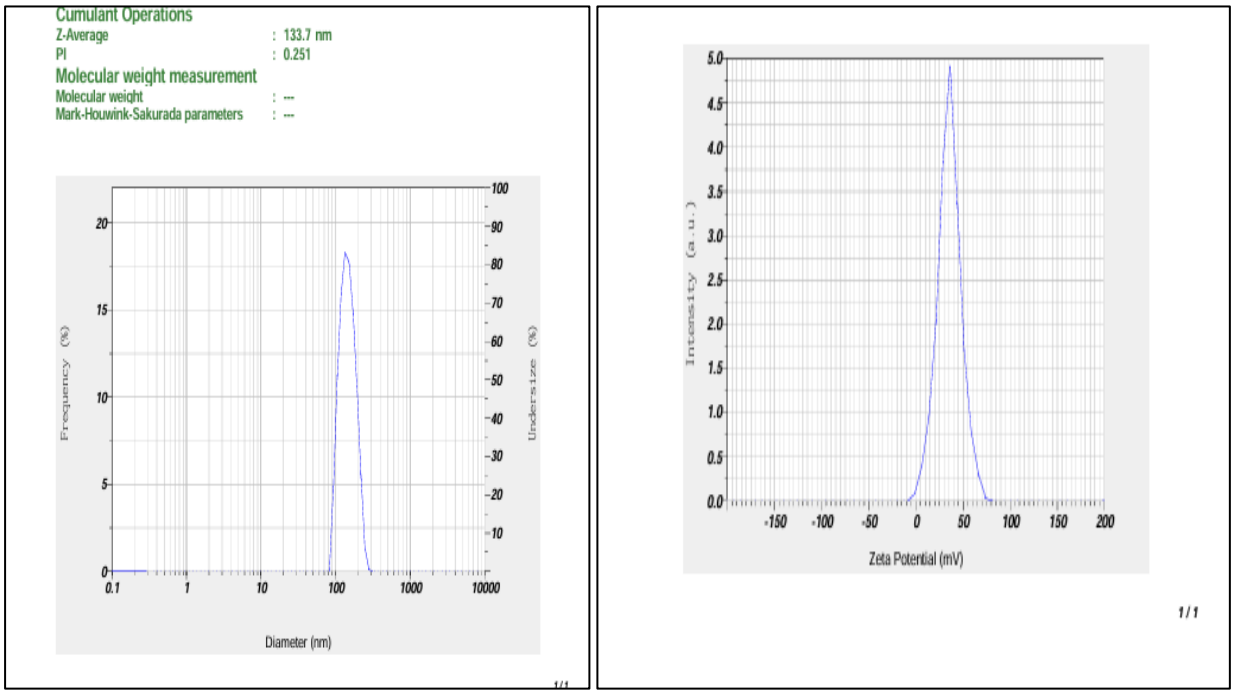

2(a) Particle Size **2(b) Zeta Potenial**

Fig 2 (a) & (b): Particle size and Zeta potential of optimized formulation (F3)

Contour plots and response surface plots for Entrapment efficiency

Polynomial equation

Entrapment Efficacy = **+85.65 + 0.8183(A) - 5.46(B) + 4.57(AB) + 0.7150(A^2) - 1.43(B^2)**.

In this equation, **A** represents the coded level of CPC and **B** represents the coded level of Cholesterol.The coded factors can be used to compare the relative impact of each factor.The negative coefficient for **B** (-5.46) indicates that as the amount of Cholesterol increases, the entrapment efficiency decreases. The positive coefficient for the interaction term AB (+4.57) shows a strong interaction between CPC and cholesterol that influences the entrapment efficiency.

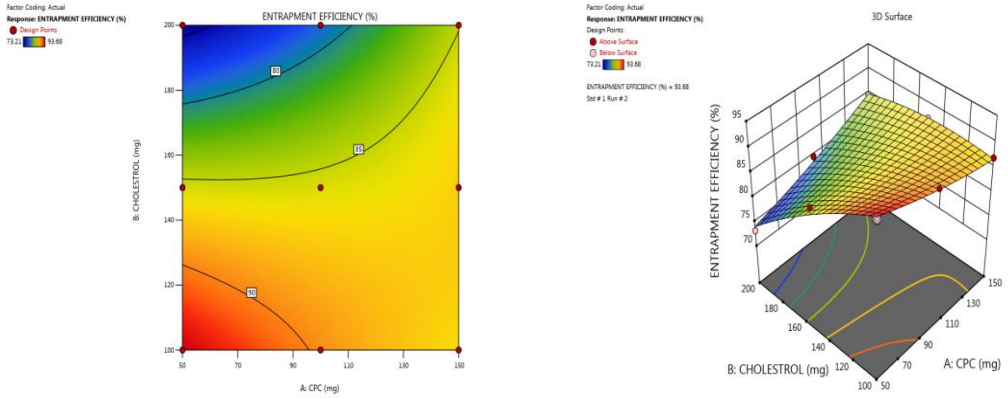

Fig 3: 2D surface plot and 3D contour plot for Entrapment Efficacy

The contour plot for Entrapment Efficiency provides a visually represents how the amounts of CPC (Factor A) and Cholesterol (Factor B) influence the final entrapment efficiency as shown in Fig3.

Relationship between Factors: The highest entrapment efficiency, represented by the red region, is found in the bottom-right corner of the plot. This region corresponds to a high concentration of CPC and a low concentration of cholesterol. Conversely, the lowest efficiency is observed in the top-left region of the plot, which signifies low CPC and high Cholesterol concentrations. The plot shows that as the cholesterol concentration increases (moving up the y-axis), the entrapment efficiency generally decreases. The ANOVA results support this, as the p-value for B- cholesterol is 0.0023 which is statistically significant ($p < 0.05$).The plot also reveals the importance of the interaction between CPC and cholesterol. While the main effect of CPC alone is not significant, its combination with cholesterol is highly influential. The contours curve shows an indicating that the relationship is not linear and that the levels of both factors must be considered together to predict the entrapment efficiency accurately. The ANOVA results support this, as the p-value for CPC (A) is 0.0238 which is statistically significant ($p < 0.05$).

The significant p-value for the interaction term (AB) in the ANOVA further supports this observation.

Table 3: Statistical analysis for Entrapment efficiency

Source	Sum of Squares	df	Mean Square	F-value	p-value	Inference
Model	271.54	5	54.31	29.08	0.0096	Significant
A-CPC	4.02	1	4.02	2.15	0.0238	
B-CHOLESTROL	178.87	1	178.87	95.77	0.0023	
AB	83.54	1	83.54	44.73	0.0068	
A^2	1.02	1	1.02	0.5475	0.5130	
B^2	4.09	1	4.09	2.19	0.2355	
Residual	5.60	3	1.87			
Cor Total	277.14	8				

Model Significance: The model's F-value is 29.08, with a p-value of 0.0096, which is less than 0.05. This indicates the model is significant, and there is only a 0.96% chance this F-value is due to noise.

Significant factor:
Factors with a p-value less than 0.05 are considered statistically significant. B (Cholesterol) shows a p-value of 0.0023, indicating it is a highly significant factor. The AB interaction term with value of 0.0068, which also falls below 0.05, making it statistically significant as well. Therefore, both B and AB significantly influence the response variable.

Fit Statistics:
The model's R^2 is 0.9798, meaning it explains approximately 97.98% of the variability in the entrapment efficiency. The Adequate Precision ratio is 17.978, which is well above the desirable value of 4, indicating an adequate signal and that the model can be used to navigate the design space.In summary, to achieve maximum entrapment efficiency, it is essential to use a high concentration of CPC in combination along with a low concentration of cholesterol.

Contour plots and response surface plots for *invitro* drug release
Polynomial equation
*Invitro*drug release = +**90.02 + 2.18(A) - 0.2167(B) - 1.27(AB) - 4.61(A^2) + 2.37(B^2)**.
In this equation, A represents the coded level of CPC and B represents the coded level of Cholesterol.The coded factors can be used to compare the relative impact of each factor.The positive coefficient for A (+2.18) indicates that as the amount of CPC increases, the drug release tends to increase. The negative coefficient for B (-0.2167) indicates that as the amount of cholesterol increases, the drug release tends to decrease, but this effect is not statistically significant. The significant quadratic and interaction terms indicates a more complex, non-linear relationship between the factors and the drug release. The *in vitro* release data from minimum to maximum represented in table 4 and 5 for all prepared nine formulations.

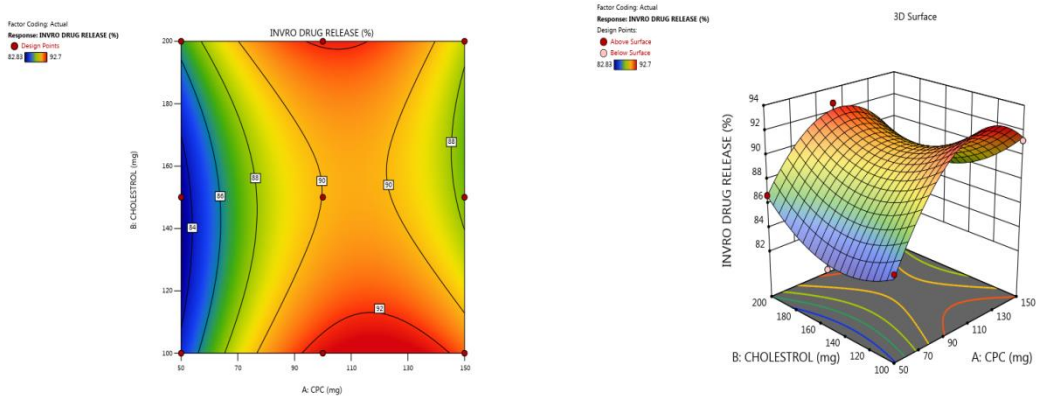

Fig4:2D surface plot and 3D contour plot for *in vitro* drug release

The contour plot for *invitro* drug release provides a visual representation of how the amounts of CPC (Factor A) and cholesterol (Factor B) influence the drug release rate.

Non-Linear Relationship: The plot's shape is distinct, showing a "saddle point" or a curved, U-shaped region. This indicates that the relationship between the factors and the response is not linear. Instead, it is best described by a quadratic model, which is consistent with the ANOVA results showing that both the A^2 (CPC squared) and B^2 (Cholesterol squared) terms are significant factors.

Effect of CPC: High drug release (indicated by the red and orange regions) is observed at both low and high CPC concentrations, especially when cholesterol concentration is also low. The plot shows a valley of lower release in the middle of the CPC range (around 90-110 mg) and peaks at the boundaries (around 50 mg and 150 mg of CPC). This non-linear effect of CPC is a key

finding from the plot.

Effect of cholesterol and Interaction: The contours are curved, suggesting an interaction between CPC and cholesterol. While the main effect of cholesterol is not significant, the quadratic term for cholesterol (B^2) is, indicating that its effect on drug release is not constant across the range. The plot shows that the highest release rates are generally associated with lower cholesterol concentrations. In summary, to achieve the highest *in vitro* drug release, should use either a very low or very high concentration of CPC, while keeping the cholesterol concentration low. The non-linear nature of the response highlights the importance of using a quadratic model to predict the outcome accurately.

Table 4: Statistical analysis for *invitro* drug release

Source	Sum of Squares	df	Mean Square	F-value	p-value	Inference
Model	89.06	5	17.81	29.72	0.0093	significant
A-CPC	28.47	1	28.47	47.51	0.0063	
B-CHOLESTROL	0.2817	1	0.2817	0.4701	0.5422	
AB	6.50	1	6.50	10.85	0.0459	
A^2	42.53	1	42.53	70.98	0.0035	
B^2	11.27	1	11.27	18.80	0.0226	
Residual	1.80	3	0.5992			
Cor Total	90.85	8				

Model Significance: The model's F-value is 29.72, with a p-value of 0.0093, which is less than 0.05. This indicates that the model is significant, and there is only a 0.93% chance this F-value is due to noise. Significant Factors: The individual factors with a p-value of less than 0.05 are considered significant.
A-CPC: Has a p-value of 0.0063, making it a significant factor.
AB (interaction term): Has a p-value of 0.0459, which is also significant.
A^2 (Quadratic term for CPC): Has a p-value of 0.0035, making it a highly significant factor.
B^2 (Quadratic term for Cholesterol): Has a p-value of 0.0226, which is also significant.

Fit Statistics:
The model's R^2 is 0.9802, meaning it explains approximately 98.02% of the variability in the *in vitro* drug release.The Adequate Precision ratio is 14.841, which are well above the desirable value of 4, indicating an adequate signal and that the model can be used to navigate the design space.

Table 5: *Invitro* release profile of posconazole loaded quatsomes(F1-F9)

Time (h)	F1	F2	F3	F4	F5	F6	F7	F8	F9
0	0	0	0	0	0	0	0	0	0
1	18.5± 0.04	19.4± 0.07	19.4± 0.21	18.1± 0.06	18.3± 0.32	10.5± 0.17	19.3± 0.17	15.1± 0.41	18.2± 0.11
2	27.3± 0.06	24.8± 0.14	21.6± 0.08	22.6± 0.09	26.6± 0.16	19.8± 0.31	25.6± 0.19	19.8± 0.21	22.8± 0.32
3	30.7± 0.03	33.2± 0.02	28.4± 0.03	35.9± 0.01	37.3± 0.11	28.4± 0.61	32± 0.28	24.1± 0.51	30.5± 0.33
4	44.2± 0.04	45.6± 0.03	35.2± 0.51	46.5± 0.02	45.8± 0.19	35.3± 0.21	44± 0.04	32.7± 0.09	39.8± 0.81
5	52.7± 0.21	55.5± 0.01	45.8± 0.06	52.8± 0.07	55.9± 0.31	48.5± 0.05	50.9± 0.01	43.6± 0.04	47.9± 0.51
6	64.6± 0.09	65.3± 0.51	54.1± 0.31	64.3± 0.09	62.1± 0.21	62.5± 0.23	65.6± 0.02	53.2± 0.49	56.5± 0.42
7	77.1± 0.04	75.8± 0.15	68.6± 0.21	75.2± 0.03	72.8± 0.05	71.4± 0.41	76.1± 0.51	68.9± 0.21	69.6± 0.28
8	89.6±0.09	84.9±0.12	92.5±0.22	86.7±0.31	92.0±0.04	87.9±0.52	91.2±0.11	88.4±0.34	82.8±0.39

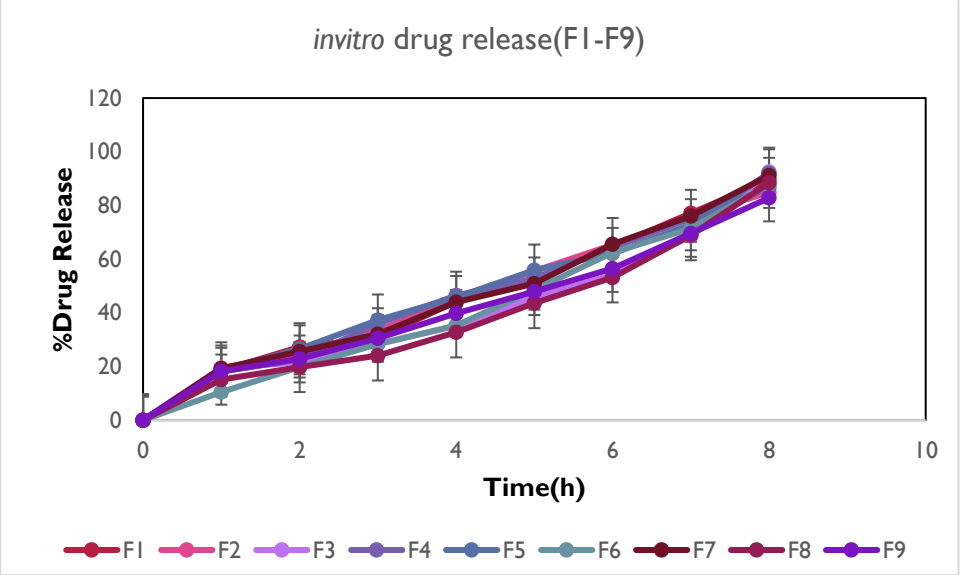

Fig5:*Invitro* release plots of posconazole loaded quatsomes(F1-F9)

***Invitro* kinetic mathematical modeling for optimized formulation (F3)**

Formulation code	Zero order	First order	Huguchi	Korsmeyer-Peppas	Hixson – Crowell
F3	0.990	0.957	0.929	0.966	0.973

The optimized formulation (F3) subjected to various kinetic modelling analysis, **formulation F3 primarily follows Zero-order release kinetics,** indicating a controlled, constant-rate release system, with followed by some supportive indications of erosion/dissolution effects from the Hixson–Crowell model.

Table 6: Statistical analysis comparison of predicted and observed values

Solution 1of 100 Response	Predicted Mean	Observed Mean	% Bias difference
Particle size (nm)	130.61	133.7	Less than 6
Entrapment Efficiency (%)	91.56	93.68	Less than 6
Invitro Drug Release (%)	95.86	92.4	Less than 6

*difference between predicted and observed should be lessthan 6%

DRUG- EXCIPIENT COMPATIBILITY STUDIES

Fourier transform infrared spectroscopy (FT-IR)

FT-IR analysis was carried out to study possible interactions between posaconazole and optimized. The spectra were recorded using a Bruker FTIR spectrophotometer in the range of 4000–400 cm^{-1} by using KBr pellet method. The pure posaconazole spectrum showed characteristic peaks at 3383 cm^{-1} (O–H stretch), 3056 cm^{-1} (C–H aromatic), 2927 cm^{-1} (C–H aliphatic), 1712 cm^{-1} (C=O stretch), 1514 cm^{-1} (C=C stretch), and 1227 cm^{-1} (C–N stretch) as shown in Fig6.

The optimized formulation containing cetylpyridinium chloride, cholesterol, and polyvinyl alcohol exhibited the same major peaks of the drug with slight shifts in intensity, indicating no significant chemical interaction and compatible drug and excipient ratio as shown in Fig7

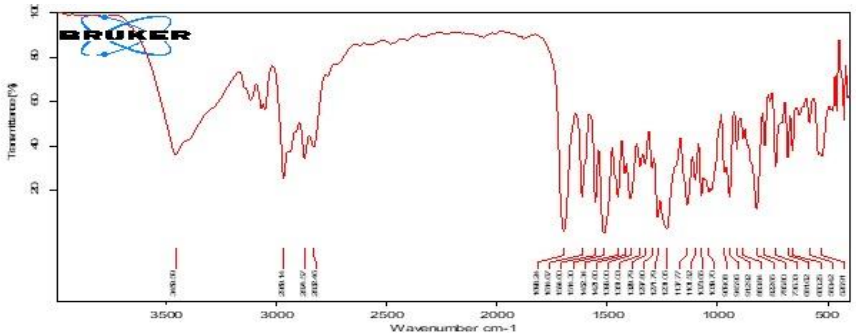

Fig.6: FT-IR spectrum of pure drug (Posaconazole)

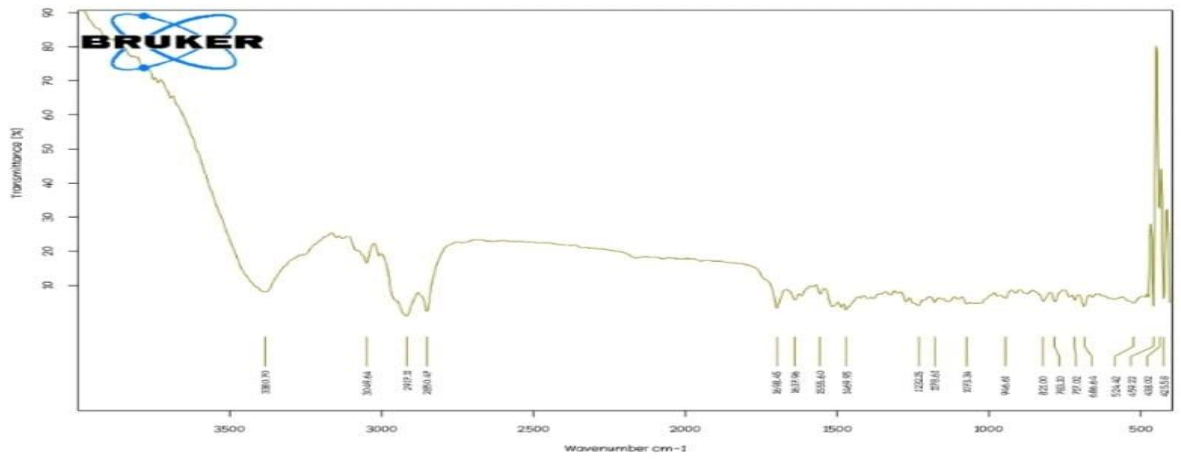

Fig.7: FT-IR spectrum of optimized formulation

X-Ray Diffraction (XRD)

The XRD pattern of pure posaconazole showed sharp and intense peaks at 2θ values around 19°, 22°, 25°, and 31°, indicating its crystalline nature. In contrast, the optimized posaconazole-loaded quatsomes exhibited broad and less intense peaks, confirming a reduction in crystallinity as shown in Fig.8 and 9**.** This indicates that the drug was successfully incorporated in the quatsomes and converted to amorphous or molecularly dispersed form which is compatible with the drug.

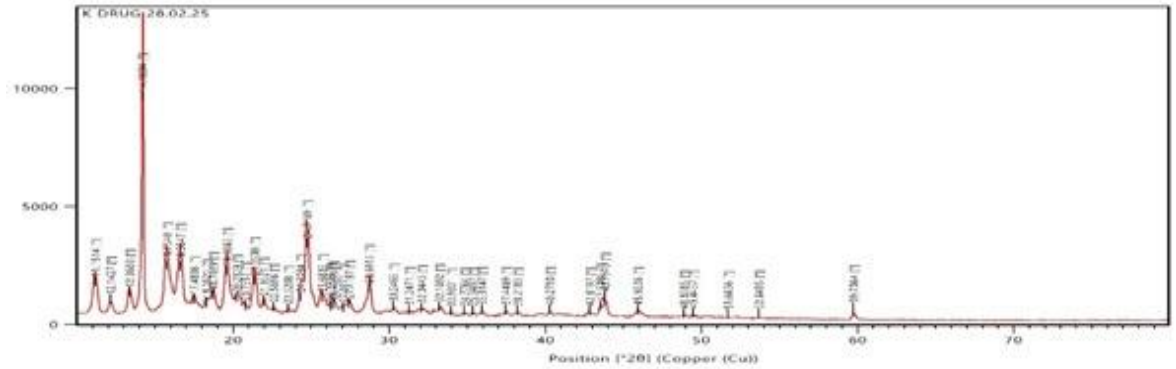

Fig.8: XRD Spectra of Pure drug (posaconazole)

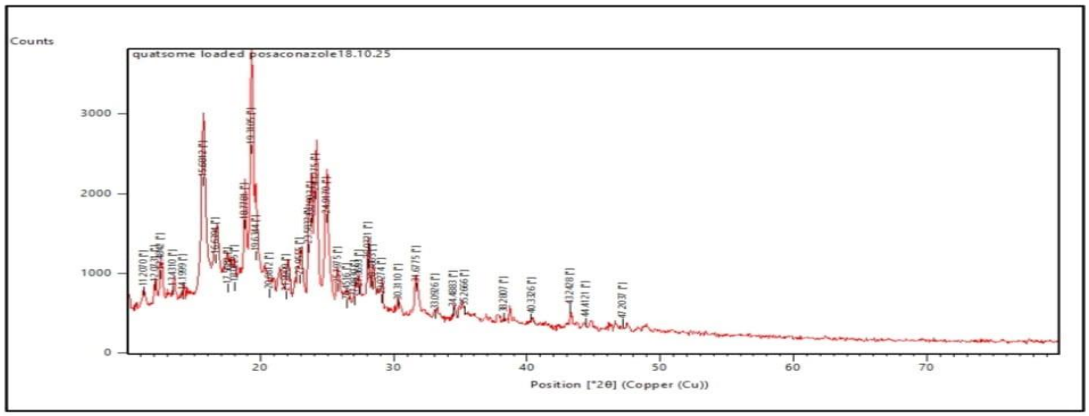

Fig.9: XRD graphs of optimized posaconazolequatsome

Differential scanning calorimetry (DSC): The DSC thermogram of pure posaconazole shows a sharp endothermic peak at 169.93 °C with an onset at 167.66 °C and end set at 172.33 °C, indicating the crystalline nature of the drug corresponding to its melting point.

The DSC thermogram of the optimized posaconazolequatsome shows a broadened, reduced-intensity peak around 169.5 °C, with additional minor transitions at lower temperatures as shown in Fig. 10 and 11. The decrease in peak sharpness and enthalpy confirms reduced crystallinity and partial amorphization of the drug due to encapsulation within the quatsome matrix.

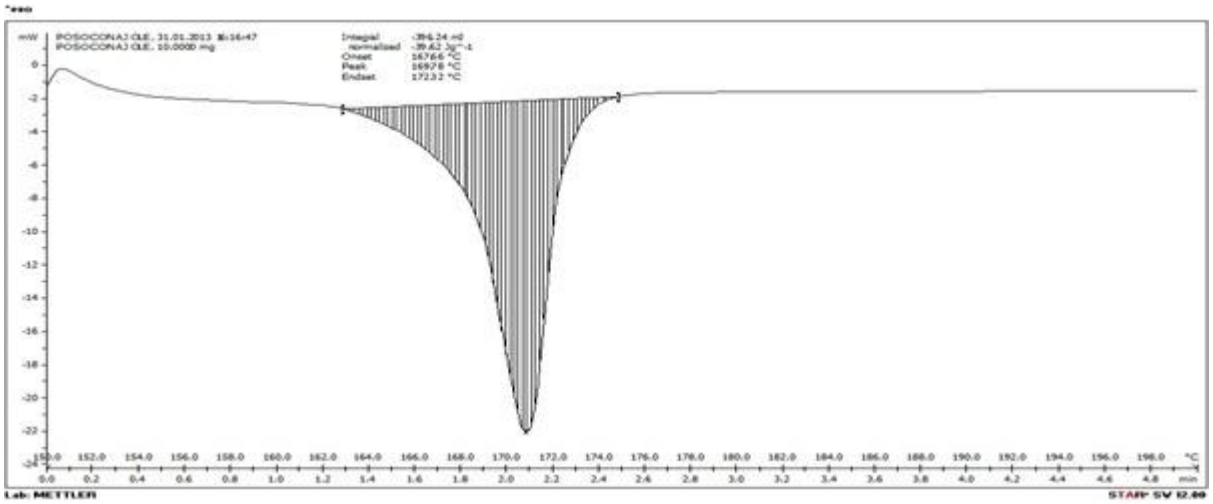

Fig.10:DSC thermogram of pure drug (Posaconazole)

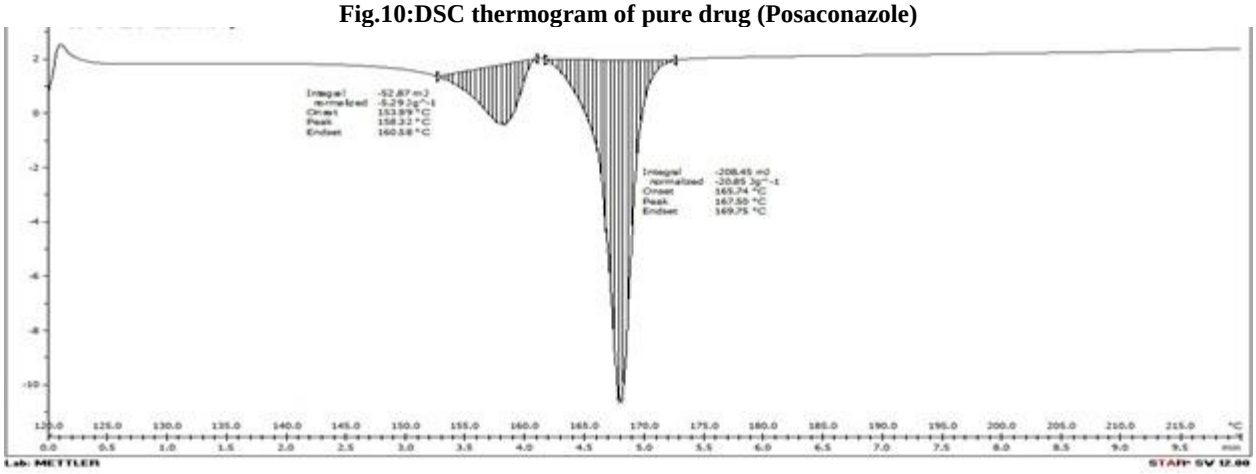

Fig.11: DSC thermogram of optimized posaconazole loaded quatsomes

Surface Morphology by Phase Contrast Microscopy

Phase-contrast microscopy of the optimized formulation of posaconazole loaded quatsomes revealed the presence of spherical, well-defined vesicular structures as shown in fig12. The vesicles appeared as bright central regions surrounded by darker circular globules, a typical optical effect produced in phase-contrast imaging due to differences in refractive index between the quatsome bilayer and the surrounding medium. This confirms the successful formation of intact quatsome vesicles without any visible aggregation or drug crystallization and successful encapsulation of drug into carrier. The uniform morphology and good dispersion indicate that the selected formulation parameters promoted stable vesicle formation. These visual observations support and demonstrating that the optimized quatsomes are structurally suitable for encapsulating drug.

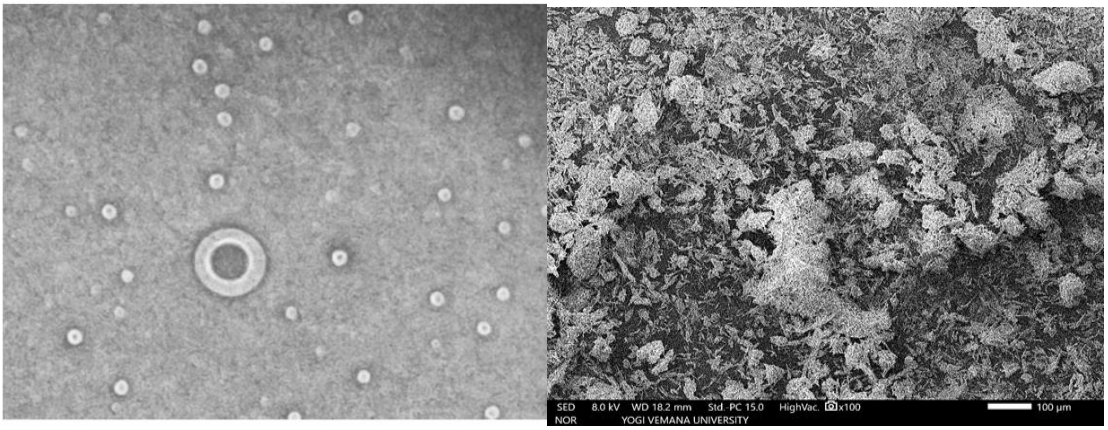

Fig.12(A):Phase Contrast Microscopy image of Optimized formulation (F3),Fig12(B):SEM image of Optimized formulation (F3)

CONCLUSION

Posaconazole-loaded quatsomes were formulated by thin film hydration method using a 3^2 factorial design with two independent variables like cetylpyridinium chloride (CPC) , cholesterol and three dependent responses; particle size, entrapment efficiency,

and in-vitro drug release. Design Expert software (version 13.0) was employed to generate nine formulations based on the selected full factorial design. Among these, formulation F3 exhibited the most desirable characteristics, with smaller particle size, higher entrapment efficiency, and superior in-vitro release, and was thus identified as the optimized formulation. The optimized batch, prepared using 100 mg of CPC and 150 mg of cholesterol, found to be a particle size of 133.7 nm, an entrapment efficiency of 93.68%, and an *in-vitro* drug release of 92.5%.Through the obtained results it was proven that quatsomes a promising and effective carrier for encapsulating poorly soluble drugs and therapeutic agents for effective delivery.

Declarations
Acknowledgment: Authors are thankful to Institute of Pharmaceutical Technology,Sri Padmavati Mahila Visvavidyalayam, DST-CURIE for providing equipments and facilities to carry out research work successfully. The author declares that financial support was received from **PM-USHA** Research grant for the research work.

Source of Funding: The author declares that financial support was received from **PM-USHA** for the research work.
Conflict of Interest: None
Competing interest: The authors declare that they have no competing interests.

REFERENCES

1. Abdel-Salam HM, El-Hady KMA. Quatsomes as a novel nanocarrier for the topical delivery of resveratrol: preparation, characterization, and *in vitro* and *in vivo* evaluation. Int J Nanomedicine. 2020;15:2451-65.**doi: 10.2147/IJN.S245906**
2. Al-Badrani SK, Al-Rubaye RR. Enhanced topical delivery of curcumin using quatsomenanovesicles for skin inflammation. J Drug DelivSci Technol. 2022;70:103211.doi:10.1016/j.jddst.2022.103211
3. Thomas N, Dong D, Richter K, Ramezanpour M, Vreugde S, Thierry B, Wormald PJ, Prestidge CA. Quatsomes for the treatment of Staphylococcus aureus biofilm. Journal of Materials Chemistry B. 2015;3(14):2770-7.doi:10.1039/C4TB01953A
4. Ferrer-Tasies L, Moreno-Calvo E, Cano-Sarabia M, Aguilella-Arzo M, Angelova A, Lesieur S. Quatsomes: vesicles formed by self-assembly of sterols and quaternary ammonium surfactants. Langmuir.2013;29(22):6519-28.doi:10.1021/la4007264
5. Aparicio C, Santos P. Cationic nanocarriers for gene delivery: quatsomes as a promising alternative. Adv Drug Deliv Rev. 2019;142:1-17.doi: 10.1016/j.addr.2018.12.009
6. Bakshi A, Gupta A. Novel vesicular systems for topical delivery of drugs: a review. J Pharm Pharmacol. 2022;74(3):321-36.doi: 10.1093/jpp/rgab176
7. Berdejo VD, Soler F. Quatsomes as effective carriers for hydrophilic and lipophilic drugs: a comparative study. Eur J Pharm Sci. 2020;145:105234.doi:10.1016/j.ejps.2020.105234
8. Grimaldi N, Andrade F, Segovia N, Ferrer-Tasies L, Sala S, Veciana J, Ventosa N. Lipid-based nanovesicles for nanomedicine. Chemical society reviews. 2016;45(23):6520-45.doi:10.1039/C6CS00566E
9. Da Silva C, Almeida P. The role of cholesterol in modulating the stability of cationic nanovesicles. Colloids Surf B Biointerfaces. 2022;210:112101.doi:10.1016/j.colsurfb.2021.112101
10. Ardizzone A, Kurhuzenkau S, Illa-Tuset S, Faraudo J, Bondar M, Hagan D, Van Stryland EW, Painelli A, Sissa C, Feiner N, Albertazzi L. Nanostructuring lipophilic dyes in water using stable vesicles, quatsomes, as scaffolds and their use as probes for bioimaging. Small. 2018 Apr;14(16):1703851.doi:10.1002/smll.20170385
11. Desai PM, Patel PB. Enhanced percutaneous absorption of a poorly soluble drug using quatsomes. J Pharm Bioallied Sci. 2021;13(2):167–74.
12. U G,Patil A, H G. Formulation and evaluation of nanoparticle drug delivery system for treatment of hypertension. Int J Appl Pharm.2023;15(6):90–97.doi:10.22159/ijap.2023v15i6.48971
13. Bordignon N, Köber M, Chinigo G, Pontremoli C, Sansone E. Quatsomes loaded with squaraine dye as an effective photosensitizer for photodynamic therapy. Pharmaceutics. 2023 Mar 10;15(3):902.doi:**10.3390/15030902**
14. Aslam-Abdul Rahiman CA, Krishnan K, Sreelekshmi AS, Arjun KK, Sreeja C Nair. NOVASOME: A pioneering advancement in vesicular drug delivery. Int J Appl Pharm. 2021;13(1):1–6. Doi:10.22159/ijap.2021v13i1.39528
15. Vargas-Nadal G, Muñoz-Úbeda M, Álamo P.Quatsomes: a stable nanovesicle platform for bio-imaging and drug-delivery applications. Nanomedicine. 2020 Feb;24:102136. doi: 10.1016/j.nano.2019.102136..
16. Hassan D, Omolo CA, Fasiku VO, Elrashedy AA, Mocktar C, Nkambule B, Soliman MES, Govender T. Formulation of pH-Responsive Quatsomes from Quaternary Bicephalic Surfactants and Cholesterol for Enhanced Delivery of Vancomycin against Methicillin Resistant *Staphylococcus aureus*. Pharmaceutics. 2020 Nov 14;12(11):1093. doi: 10.3390/pharmaceutics12111093.
17. Sinico C, Fadda AM. Vesicular carriers for dermal drug delivery. Expert Opin Drug Deliv. 2009 Aug;6(8):813-25. doi: 10.1517/17425240903071029.
18. Gupta R, Sharma M. Lipid-based nanocarriers for topical delivery of drugs: a review. Eur J Pharm Biopharm.2022;174:145-60.doi:10.22270/jddt.v13i4.5781
19. Mancuso A, Cristiano MC, Fresta M, Paolino D. The Challenge of Nanovesicles for Selective Topical Delivery for Acne Treatment: Enhancing Absorption Whilst Avoiding Toxicity. Int J Nanomedicine. 2020 Nov 19;15:9197-9210. doi: 10.2147/IJN.S237508.
20. Köber M, Illa-Tuset S, Ferrer-Tasies L.Stable nanovesicles formed by intrinsically planar bilayers. J Colloid Interface Sci. 2023 Feb;631(Pt A):202-211. doi: 10.1016/j.jcis.2022.10.104.
21. Fatouros DG, Lamprou DA, Urquhart AJ, Yannopoulos SN, Vizirianakis IS. Lipid-like self-assembling peptide nanovesicles for drug delivery. ACS applied materials interfaces. 2024 Jun 11;6(11):8184-9.

22. Ibrahim SA, El-Dardiry M. Cationic surfactants in vesicular systems: a review. Drug Discov Today. 2020;25(5):785–94.
23. Farzaneh H, Ebrahimi Nik M, Mashreghi M, Saberi Z, Jaafari MR, Teymouri M. A study on the role of cholesterol and phosphatidylcholine in various features of liposomal doxorubicin: From liposomal preparation to therapy. Int J Pharm. 2018 Nov 15;551(1-2):300-308. doi: 10.1016/j.ijpharm.2018.09.047.
24. Jain A, Kumar P. Nanotechnology-based drug delivery systems for psoriasis: current status and future perspectives. Expert Opin Drug Deliv. 2021;18(10):1485–501.
25. Johnson AM, Williams P. Quatsomes: an overview of their properties and potential applications. AdvTher. 2019;2(1):1-12.
26. Liu X, Wu H. The effect of cholesterol on the stability of cationic nanovesicles: a molecular dynamics study. Nanoscale. 2020;12(35):18195-206.
27. Chaurasia G, Lariya N. A comparative assessment of vesicular formulations: Transfersomesand conventional liposomes loaded ivabradine hydrochloride. Int J Appl Pharm. 2020;12(6):51-55. doi:10.22159/ijap.2020v12i6.39391
28. Gupta RD, Sharma V. Quality by design driven formulation development and optimizationof poor soluble anti-hypertensive drug for improved solubility. Int J Appl Pharm.2025;17(4):231-240. doi:10.22159/ijap.2025v17i4.53836.
29. Tomar S, Kumar YK. Development of hydrogel formulations of selected antifungal drugs using cyclodextrin based nanosponges as a carrier. Int J Appl Pharm. 2025; 17(3):157–169. doi.org/10.22159/ijap.2025v17i3.5230
30. Li D, Martini N, Liu M, Falconer JR, Locke M, Wu Z, Wen J. Non-ionic surfactant vesicles as a carrier system for dermal delivery of (+)-Catechin and their antioxidant effects. J Drug Target. 2021 Mar;29(3):310-322. doi: 10.1080/1061186X.2020.1835923. Epub 2020 Oct 27. PMID: 33044095.
31. Preethi GB, Jain AP. Polymeric nanoparticles of loratadinebetacyclodextrin inclusion complex: 3^2 factorial design, optimization and *in-vitro* evaluation. Int J Drug Deliv Technol. 2025;15(3):934-40. doi:10.25258/ijddt.15.3.4.
32. Lam HT, Le-Vinh B, Phan TNQ, Bernkop-Schnürch A. Self-emulsifying drug delivery systems and cationic surfactants: do they potentiate each other in cytotoxicity? J Pharm Pharmacol. 2019 Feb;71(2):156-166. doi: 10.1111/jphp.13021.